Green synthesis of lead oxide nanoparticles, characterization and adsorption study for removal of malachite green dye

Abstract:

In this study lead oxide nanoparticles were synthesized by using ecofriendly and non-toxic Morus rubra extract. The obtained lead oxide nanoparticles were characterized by XRD, SEM, EDX, BET and FTIR techniques. Powder X-ray diffraction analysis revealed that synthesized PbO nanoparticles had crystallite structure of high purity. SEM survey shows that the obtained nanoparticles having in general uniform particle distribution and the particle sizes vary within the range of 22.4 to 29.2nm. As established by EDX to confirm the presence of lead and oxygen, the weight percentage of the latter was (71.5 % Pb and 28.5% O), respectively. FT-IR spectra exhibit a sharp peak at 439.38 and 595.46 cm^{-1} attributed to PbO vibration, confirming the formation of PbO nanoparticles. The effectiveness of PbO nanostructures for removing indigo carmine (MG) dye from an aqueous solution is demonstrated in this article. , the MG dye uptake and adsorption processes were investigated using a PbO sorbent. The maximum adsorption capacity and contact time were optimized which corresponding to 41.3 mg. g^{-1} and 60min respectively.

Keywords: Morus rubra extract, PbO nanoparticles, MG dye removal, Adsorption, contact time.

1. Introduction:

Nanotechnology and nanobiotechnology are growing rapidly, especially in the area of nanoparticle synthesis [1, 2]. Nanotechnology is currently employed as a crossover technology in electrical appliances [3], construction [4], and composite materials [5], as well as consumer goods [6]. Due to their small size and high surface-to-volume ratio, nanostructures have attracted considerable interest, and their physicochemical properties can be separated from those of bulk materials.[7-10]. Metal oxide nanoparticles are a promising tool for biomedical applications due to their high stability, simple manufacturing techniques, porosity, and their ability to be easily incorporated into hydrophobic and hydrophilic systems due to their negatively charged surface[11-13].

Lead oxide (PbO) is a significant industrial substance that has been widely used in batteries[14], pigments[15], and the glass industry[14]. They are widely used in construction skeletons, and road construction due to their anti-rust, anti-bacterial, and anti-algal characteristics[16-18]. The semiconductor PbO exists in two crystalline forms: litharge (tetragonal crystalline structure) and massicot (orthorhombic crystalline structure).[19, 20]. It has been established that the -PbO form of litharge crystals is stable at low temperatures, whereas the -PbO form of massicot crystals appears to be stable at high temperatures. [21, 22]. PbO nanostructures were manufactured utilizing multiple techniques, including thermal breakdown[23, 24], Sol–gel pyrolysis[21, 25], thermal decomposition under microwave radiation[16, 26], chemical deposition[16, 27], and solvothermal methods[28].

Since lead pollution has a significant influence on the ecosystem, it is necessary to identify solutions. Metal oxide nanoparticles may be manufactured through nanotechnology and biosynthesis[29, 30]. The biosynthesis of nanoscale lead oxide (PbO-NPs) could increase its properties while reducing the amount of hazardous substances needed in its synthesis[31, 32]. In this study, PbO-NPs were synthesized utilizing Morus rubra extract, and the effect of preparation method on malachite green dye adsorption was examined.

2. Experimental methods

2.1 Synthesis of PbO-NPs

The biosynthesis of PbO-NPs involved the use of Morus leaf extract as coating agents. The leaves of Morus were weighed (4g) and washed with distilled water before being put to 100 cc of distilled water and allowed to boil for 15 minutes before being filtered and placed in a water bath at 65 ° C for 120 minutes until a clear and yellow solution was produced. Thereafter, 5g of Pb (NO3)2 was added slowly to the solution, which was agitated in a water bath at 80 °C until a resin with a yellow hue was created. Resin was dried in an oven at 90°C for two hours before being roasted at 500°C for 90 minutes. The observed result was an orange powder known as PbO-NPs.

2.2 Adsorption studies:

The adsorption experiments were performed using malachite green (MG) as the standard dye. MG is a triarylmethane chloride dye that is essentially a cationic dye. Its

IUPAC name is 4-4-dimethylaminophenyl-phenylmethylidene-1-cyclohexa-2,5-dienylidene-dimethyl azanium chloride. C_6H_5 [CC_6H_4] $(CH_3)_2Cl$ with a molecular weight of 327. The dye's deep blue color is a result of its significant absorption in the visible area at 618 nm. To prevent photolysis, batch adsorption procedures were undertaken at room temperature in foil-lined glass beakers with a 350rpm magnetic stirrer. The standard concentration of malachite green was established to be 10 ppm, and various aliquots of the experimental sample were collected from this concentration. Before and after each experiment, the concentration of malachite green was determined using a UV–Vis absorption spectrophotometer to measure the visible absorbance. The following calculation can be used to compute the amount of IC adsorbed per gram of nanoparticles at time (min) using the following equation (1).

$$qt = (C0 - Ct)\frac{V}{m}$$

Where C_0 and C_t are the initial and equilibrium concentrations of the dye, V is the dye solution volume, and m is the adsorbent's mass.

2.3 Characterization of PbO NPs:

The produced PbO nanoparticles were studied by x-ray diffraction (XRD), energy dispersive x-ray (EDX), scanning electron microscopy (SEM), UV– Visible spectrometer, Brunauer Emmett Teller analyzer (BET), and Fourier transform infrared spectroscopy (FT-IR). Muffle furnace was employed for calcination, and the powder's XRD patterns were examined to determine the phase structure and average crystallite size of PbO-NPs nanoparticles. Using Cu–K radiation (= 0.15406 nm) and a diffractometer (D8 Advance Bruker, Mannheim, Germany), the samples were recorded. Using SEM – EDX, the structural shape and chemical composition of PbO nanoparticles were analyzed and evaluated. Before to being baked in an oven at 105 °C, the specimens were covered with a thin layer of gold to induce electrical conductivity on the surface of the PbO-powder. The mode of chemical bonding in the produced materials was investigated by FTIR (Nicolet 6700, The mode Fisher, Waltham, MA, USA) in the 4000–400 cm^{-1} range with a resolution of 4 cm^{-1}. Using N_2 adsorption-desorption isotherms at the N_2 boiling point (77 K) and ASAP 2020 (Micromeritics) equipment, the porosity of the samples was evaluated. Before the adsorption experiment, the specimen was degassed with Helium at 250 ^0C for two hours to eliminate moisture and adsorbed impurities. Using the BET (Brunauer,

Emmons, and Teller) formula and the t-plot approach of Lippens and de Boer, the porosity and surface area were estimated.

3. Results and discussions

3.1 Scanning electron microscopy (SEM)

The size shape and rearrangement of the product PbO nanoparticles has been investigated by scanning electron microscopy (SEM). The SEM image of the produced nanoparticles reveals that the particles are nanoscale and distributed uniformly.. The particle size observed in the SEM image is in the range of 22.4- 29.2 nm, which is good agreement with this estimator.

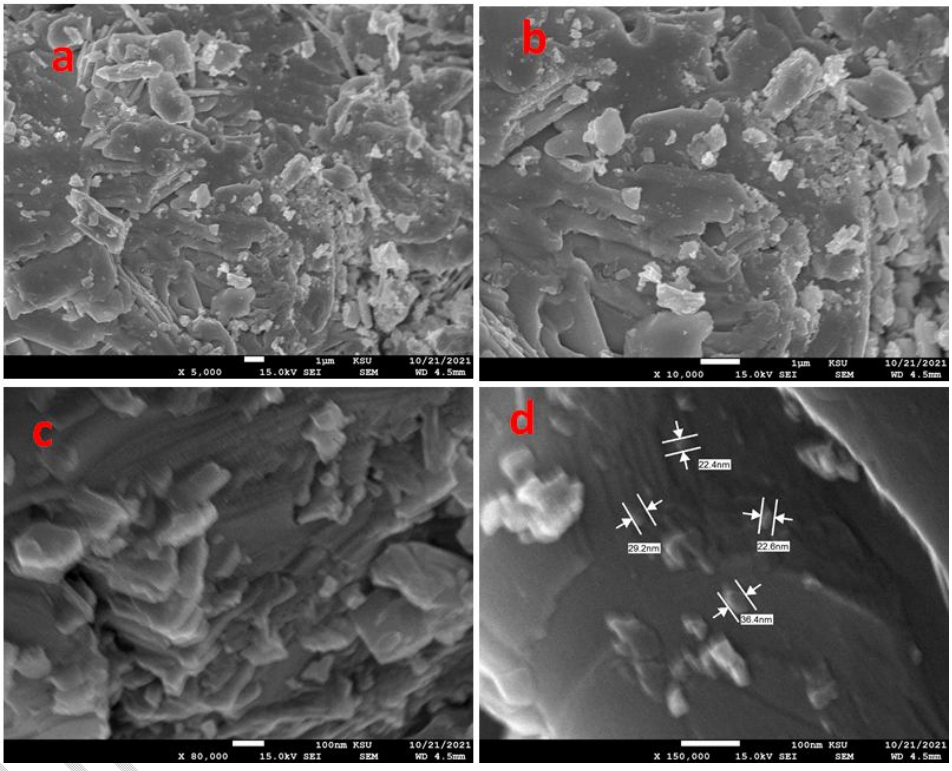

Figure (1): SEM image of PbO nanoparticles at different magnification

3.2 Energy dispersive x-ray spectra (EDX)

At 15keV, an EDX study was performed on PbO-NPs. PbO-NPs were found to include lead (Pb) and oxygen (O), according to the results. Based on EDX examination, the weight percent of Lead and oxide were calculated to be O: 28.5 weight% and Pb: 71.5 weight%, respectively. The EDX spectra contained no other elemental contaminants. In PbO, the EDX analysis revealed a homogeneous distribution of lead to oxygen with a 3:1 atomic ratio. This result revealed that pure

PbO-NPs were formed. The sample's elemental analysis indicates that the produced material was Lead oxide.

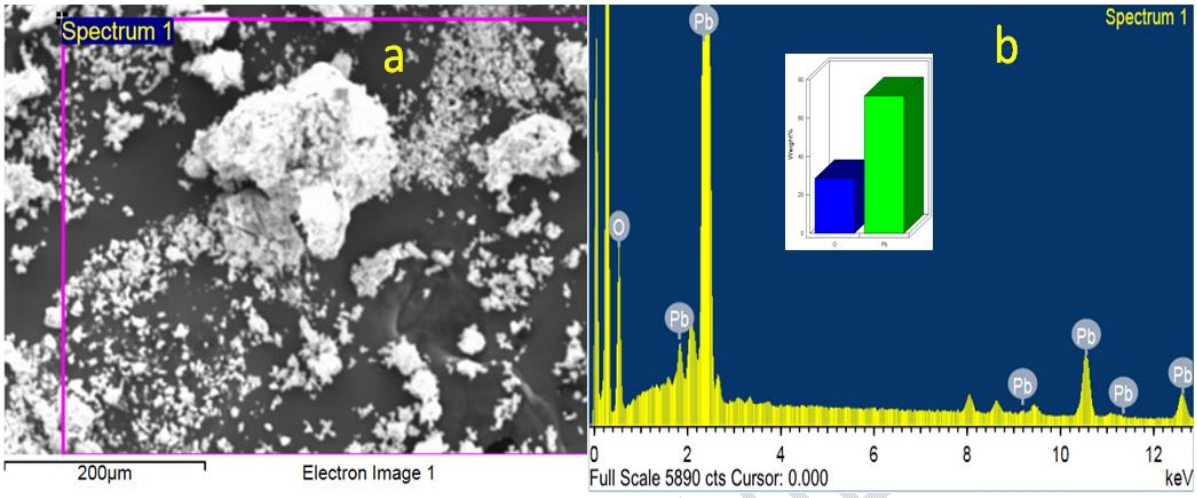

Figure (2): (a) FE-SEM of PbO NPs (b) EDX analysis and percent composition of PbO nanoparticles

3.3 X-ray diffraction (XRD)

The structural analysis of the powder material is analyzed by X-Ray diffraction is illustrated in Figure (3). The obtained XRD results are compared to the JCPDS card (88-1589)[33]. Here, Fig.5 displays a significant peak, which corresponds to the (1, 1) plane, indicating that PbO is highly crystalline.

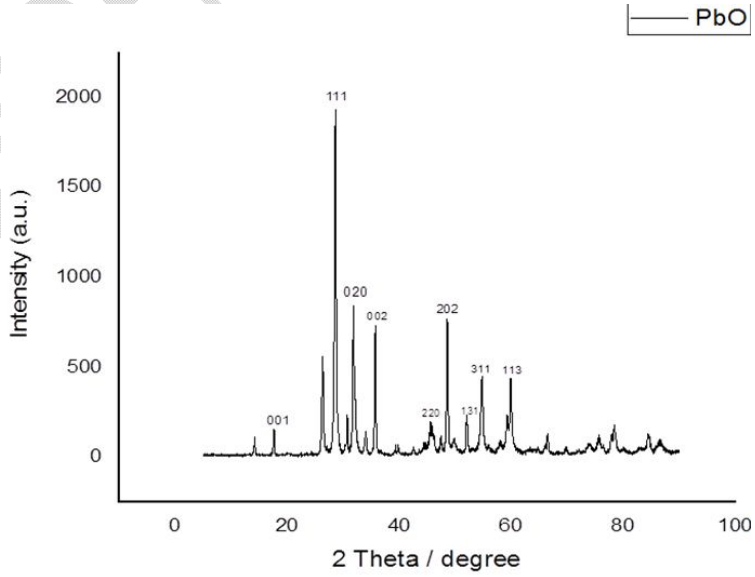

Figure (3): XRD analysis of PbO nanoparticles

3.4 Functional group analysis (IR)

Functional group analysis of PbO-NPs nanoparticles is shown in Fig.4. FTIR spectra were recorded in solid phase using the KBr pellet technique in the range of 4000-400 cm^{-1}. FTIR examination of green produced PbO-NPs exhibited vibrational peaks at 429.42 and 530.21 cm1, verifying the synthesis of very pure PbO-NPs nanoparticles. The sharp peak observed at 1384.25 cm^{-1} is attributed to Pb-O stretching vibrations. The peak around 3444.26 cm^{-1} show the presence of - OH stretching of hydroxyl groups due to moisture.

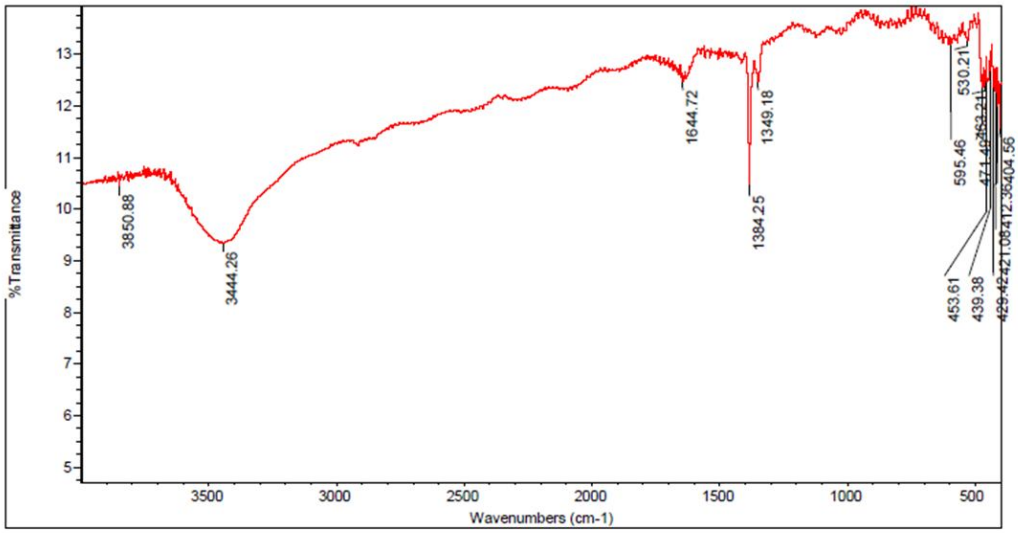

Figure (4): IR spectrum of PbO nanoparticles

3.5 The surface area (BET):

Nanomaterials can be identified by their specific surface area, which is one of the primary indicators of their nanoparticle content. PbO NPs were characterized by their surface area (BET). The approach is based on constant-temperature single-gas adsorption. As an adsorbate on the surface of PbO NPs, nitrogen gas was utilized. Brunauer Emminger Teller (BET) and Barrett Joyner Halenda (BJH) diagrams were used to evaluate the surface texture parameters of PbO. Based on the N_2 sorption isotherm, the isotherm is of Langmuir type IV (Fig. 6a), with a relative pressure (P/Po = 0.0-0.99). In addition, the hysteresis loop is type H3 (Fig. 6b), confirming that the nanoparticles with slit-shaped pores are mesoporous. The results indicate that PbO NPs have a surface area of 2.975m^2/g, which is a considerable value. In addition, the pore volume and radius are 0.007 cc/g and 15.934A^0, respectively.

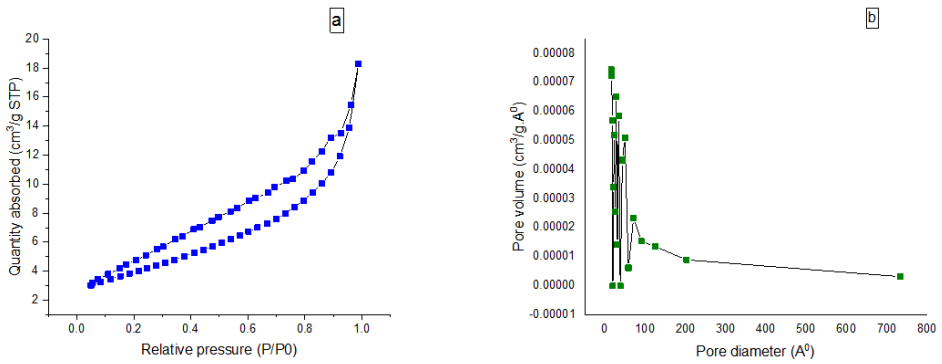

Figure (5): (a) (BET) and N_2 adsorption –desorption isotherm (b) (BJH) pore size distribution of the PbO nanoparticles sample

3.6 Adsorption study and contact time

Lead oxide nanocomposites were utilized as an adsorbent to evaluate MG adsorption. One of the most important parameters influencing the design of a polluted water treatment system is the equilibrium contact time. Figure 6 illustrates the effect of equilibrium time on MG dye adsorption. It can be observed that, in the early stages of the adsorption process, adsorption was rapid before approaching equilibrium gradually. The contact time and equilibrium adsorption capacity qe were around 60 minutes and 41.3mg/g at an MG dye concentration of 10 ppm, and a fast adsorption equilibrium time is advantageous for applications requiring rapid adsorption.

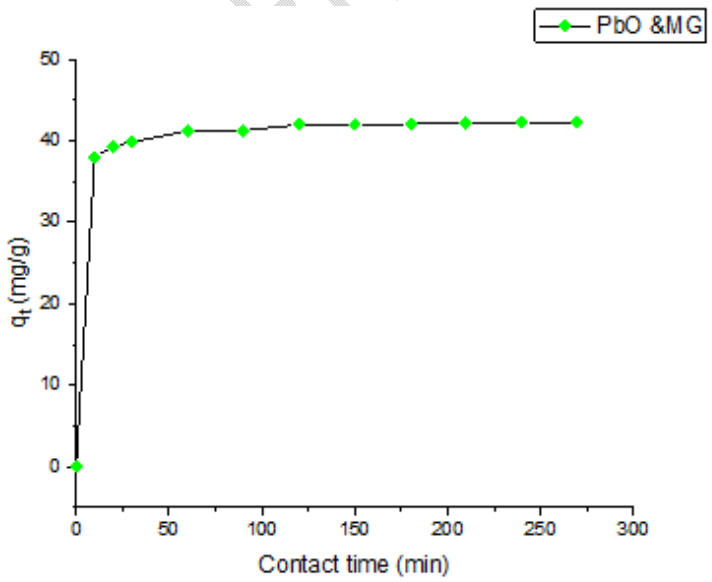

Figure (6): Adsorption capacity of PbO at different contact time

Conclusion:

PbO-NPs is one of the most widely utilized metal nanoparticles in industry. Throughout this investigation, lead oxide nanoparticles were effectively manufactured using the simple, inexpensive, and nontoxic sol-gel approach. SEM, EDX, XRD, BET analysis and FTIR-Spectroscopy characterization technique confirm the result. XRD and FTIR confirmed the crystalline nature and existence of PbO nanoparticles. The formation was supported by SEM images with the diameter of 22.4- 29.2 nm. The adsorption investigation demonstrates the efficacy and application of PbO nanoparticles as a sorbent for MG dye removal. The results indicated that MG dye adsorption was relatively rapid as equilibrium was reached in 60 minutes with an adsorption capacity of 41,3 mg. g-1.

References:

1. Kumar, A., et al., *A rationalized and innovative perspective of nanotechnology and nanobiotechnology in chronic wound management.* 2020. **60**: p. 101930.
2. Nagpure, G., et al., *Nanobiotechnology for livestock breeding technologies*, in *Nanobiotechnology for the Livestock Industry*. 2023, Elsevier. p. 233-242.
3. Kuda, A. and M.J.M.T.P. Yadav, *Opportunities and challenges of using nanomaterials and nanotechnology in architecture: An overview.* 2022.
4. Abdin, A.R., A.R. El Bakery, and M.A.J.A.S.E.J. Mohamed, *The role of nanotechnology in improving the efficiency of energy use with a special reference to glass treated with nanotechnology in office buildings.* 2018. **9**(4): p. 2671-2682.
5. Bashir, S., et al., *Synergistic effects of doping, composite formation, and nanotechnology to enhance the photocatalytic activities of semiconductive materials.* 2023. **135**: p. 113264.
6. Kuiken, T., et al., *Public's Understanding, Perceptions, and Acceptance of Nanotechnology through the Lens of Consumer Products*, in *Nanoengineering*. 2015, Elsevier. p. 151-171.
7. Liu, Q., et al., *Physicochemical and in vitro digestion properties of soy isoflavones loaded whey protein nanoparticles using a pH-driven method.* 2022. **82**: p. 103209.
8. Erfani, A., M.K. Pirouzifard, and S.J.F.C. Pirsa, *Photochromic biodegradable film based on polyvinyl alcohol modified with silver chloride nanoparticles and spirulina; Investigation of physicochemical, antimicrobial and optical properties.* 2023: p. 135459.
9. Liu, Q., et al., *Physicochemical properties of nanoparticles affecting their fate and the physiological function of pulmonary surfactants.* 2021.
10. Huang, Y., et al., *Improving kidney targeting: The influence of nanoparticle physicochemical properties on kidney interactions.* 2021. **334**: p. 127-137.
11. Alavi, M., et al., *Metal and metal oxide-based antiviral nanoparticles: Properties, mechanisms of action, and applications.* 2022: p. 102726.
12. Ahmad, S., et al., *Diverse comparative studies for preferential binding of graphene oxide and transition metal oxide nanoparticles.* 2022. **647**: p. 129057.

13. Patil, S.P., R.Y. Chaudhari, and M.S.J.T.O. Nemade, *Azadirachta indica leaves mediated green synthesis of metal oxide nanoparticles: A review.* 2022: p. 100083.
14. Tao, D., et al., *PbO nanoparticles anchored on reduced graphene oxide for enhanced cycle life of lead-carbon battery.* 2022. **432**: p. 141228.
15. Mehrabi, N., et al., *Application of deep eutectic solvent for conjugation of magnetic nanoparticles onto graphene oxide for lead (II) and methylene blue removal.* 2020. **8**(5): p. 104222.
16. Bratovcic, A.J.L.C., *Synthesis, characterization, applications, and toxicity of lead oxide nanoparticles.* 2020. **6**: p. 66.
17. Soltanian, S., et al., *Biosynthesis of zinc oxide nanoparticles using hertia intermedia and evaluation of its cytotoxic and antimicrobial activities.* 2021. **11**: p. 245-255.
18. Kumar, N., et al., *TiO 2 and its composites as promising biomaterials: a review.* 2018. **31**: p. 147-159.
19. Miri, A., et al., *Biosynthesis and cytotoxic activity of lead oxide nanoparticles.* 2018. **11**(4): p. 567-572.
20. Kelaidis, N., et al., *Vapor–liquid–solid growth and properties of one dimensional PbO and PbO/SnO 2 nanowires.* 2022. **3**(3): p. 1695-1702.
21. Elawam, S., et al., *Characterizations of beta-lead oxide "massicot" nano-particles.* 2016. **17**(1): p. 1-10.
22. Noukelag, S., et al., *Bio-inspired synthesis of PbO nanoparticles (NPs) via an aqueous extract of Rosmarinus officinalis (rosemary) leaves.* 2021. **36**: p. 421-426.
23. Ranjbar, M. and M. Yousefi, *Sonochemical synthesis and characterization of a nano-sized lead (II) coordination polymer; a new precursor for the preparation of PbO nanoparticles.* 2016.
24. Mahmoud, M.E., et al., *Design and testing of high-density polyethylene nanocomposites filled with lead oxide micro-and nano-particles: Mechanical, thermal, and morphological properties.* 2019. **136**(31): p. 47812.
25. Marouzi, S., Z. Sabouri, and M.J.C.I. Darroudi, *Greener synthesis and medical applications of metal oxide nanoparticles.* 2021. **47**(14): p. 19632-19650.
26. Nafees, M., M. Ikram, and S.J.A.N. Ali, *Thermal stability of lead sulfide and lead oxide nano-crystalline materials.* 2017. **7**: p. 399-406.
27. Akay, D., U. Gökmen, and S.B.J.P.S. Ocak, *Structural role of double layer amphoteric oxides forms on electrical conductivity: PbO/zinc oxide semiconductor.* 2022. **97**(9): p. 095803.
28. Darki, S.Y., et al., *Effects of PVP surfactant and different alkalis on the properties of PbO nanostructures.* 2021. **262**: p. 124305.
29. Bouafia, A. and S.E.J.M.-R.i.O.C. Laouini, *Plant-mediated synthesis of iron oxide nanoparticles and evaluation of the antimicrobial activity: a review.* 2021. **18**(6): p. 725-734.
30. El Shafey, A.M.J.G.P. and Synthesis, *Green synthesis of metal and metal oxide nanoparticles from plant leaf extracts and their applications: A review.* 2020. **9**(1): p. 304-339.
31. Trivedi, R., et al., *Recent Advancements in Plant-Derived Nanomaterials Research for Biomedical Applications.* 2022. **10**(2): p. 338.
32. OSMAN, A.F., et al., *CHARACTERIZATION OF LEAD OXIDE MILLED NANOPARTICLES AND THE EFFECT OF THEIR INCORPORATION ON THE THERMAL PROPERTIES OF POLYSTYRENE.* 2023. **18**(1): p. 481-507.
33. Mythili, N. and K.J.I.J.S.E.R. Arulmozhi, *Characterization studies on the chemically synthesized α and β phase PbO nanoparticles.* 2014. **5**(1): p. 412-416.